Published in final edited form as:
J Mol Biol. 2007 October 5; 372(5): 1123–1136.

Structures of MART-1$_{26/27–35}$ Peptide/HLA-A2 Complexes Reveal a Remarkable Disconnect between Antigen Structural Homology and T Cell Recognition

Oleg Y. Borbulevych[1,2], **Francis K. Insaidoo**[1], **Tiffany K. Baxter**[1], **Daniel J. Powell Jr**[3], **Laura A. Johnson**[3], **Nicholas P. Restifo**[3], and **Brian M. Baker**[1,2,*]

1 *Department of Chemistry and Biochemistry, 251 Nieuwland Science Hall, University of Notre Dame, Notre Dame IN 46556, USA*

2 *Walther Cancer Research Center, 251 Nieuwland Science Hall, University of Notre Dame Notre Dame, IN 46530, USA*

3 *National Cancer Institute, National Institutes of Health Bethesda, MD 20892, USA*

Abstract

Small structural changes in peptides presented by major histocompatibility complex (MHC) molecules often result in large changes in immunogenicity, supporting the notion that T cell receptors are exquisitely sensitive to antigen structure. Yet there are striking examples of TCR recognition of structurally dissimilar ligands. The resulting unpredictability of how T cells will respond to different or modified antigens impacts both our understanding of the physical bases for TCR specificity as well as efforts to engineer peptides for immunomodulation. In cancer immunotherapy, epitopes and variants derived from the MART-1/Melan-A protein are widely used as clinical vaccines. Two overlapping epitopes spanning amino acid residues 26 through 35 are of particular interest: numerous clinical studies have been performed using variants of the MART-1 26–35 decamer, although only the 27–35 nonamer has been found on the surface of targeted melanoma cells. Here, we show that the 26–35 and 27–35 peptides adopt strikingly different conformations when bound to HLA-A2. Nevertheless, clonally distinct MART-1$_{26/27–35}$-reactive T cells show broad cross-reactivity towards these ligands. Simultaneously, however, many of the cross-reactive T cells remain unable to recognize anchor-modified variants with very subtle structural differences. These dichotomous observations challenge our thinking about how structural information on unligated peptide/MHC complexes should be best used when addressing questions of TCR specificity. Our findings also indicate that caution is warranted in the design of immunotherapeutics based on the MART-1 26/27–35 epitopes, as neither cross-reactivity nor selectivity is predictable based on the analysis of the structures alone.

Keywords

peptide/MHC; crystal structure; cross-reactivity; specificity; Melan-A; MART-1

Although structural studies of peptide/major histocompatibility complex (MHC) molecules and their interactions with αβ T cell receptors have considerably advanced our understanding of the molecular details of cellular immunity, the relationships between peptide/MHC structure and TCR specificity and cross-reactivity remain elusive. Alterations to antigenic peptides that result in very minor structural changes often result in substantial changes in immunological

*E-mail address of the corresponding author: bbaker2@nd.edu.
Edited by I. Wilson

potency,[1–5] leading to the commonly-held notion that T cell receptors can be exquisitely sensitive to antigen structure. Yet there are striking exceptions to this observation. Lee *et al.* recently demonstrated efficient TCR recognition of native and variant HIV gag epitopes that have significant structural differences across the center of the peptide.[6] Gagnon *et al.* showed TCR cross-reactivity between the native HTLV-1 $Tax_{11–19}$ peptide and a variant with a modified P5 side-chain that imparts dramatic structural differences on the peptide.[7] More remarkably, Zhao *et al.* identified a murine T cell clone that recognizes the peptide p1027 (FAPGVFPYM) presented by H-2D^b as well as the peptide p1049 (ALWGFFPVL) peptide presented by human HLA-A*0201 (HLA-A2).[8] These structural studies build on the functional studies reported by Hemmer *et al.*, who identified T cell clones that cross-react with ligands sharing minimal sequence or chemical homology.[9] The resulting unpredictability of how T cells will respond to different or modified peptides has implications for our understanding of the physical bases for TCR specificity and cross-reactivity, and impacts the design and use of variant peptides with altered immunological potencies.

The epitopes spanning amino acid residues 26–35 and 27–35 from the MART-1/Melan-A protein, highly expressed in melanoma cells, provide a prime example of T cell recognition of multiple peptides and the use of peptide variants designed to elicit altered immunological responses. Initial studies identified the 27–35 nonamer (AAGIGILTV, referred to as AAG; see Table 1) as the immunodominant epitope of the MART-1 protein,[10,11] although the 26–35 decamer (EAAGIGILTV, referred to as the EAA decamer), was also found to be recognized by MART-1-reactive T cells.[10] A later study comparing the two peptides indicated that the EAA decamer had equal or improved immunonogenicity compared to the AAG nonamer and bound more tightly to the restricting MHC molecule, HLA-A2.[12] Modification of the EAA decamer with leucine at position 2 (E**L**AGIGILTV, referred to as the ELA decamer) resulted in even better binding to HLA-A2 and more potent immunogenicity.[13] On the other hand, modification of the native AAG nonamer with leucine at position 2 (A**L**GIGILTV; ALG nonamer) greatly reduced or abolished CTL recognition compared to the AAG nonamer, despite improving HLA-A2 binding. This observation led to the suggestion that the Ala2→Leu modification in the AAG nonamer altered the conformation of the peptide in the HLA-A2 peptide-binding groove,[13] presumably away from a common conformation shared between the EAA and ELA decamers and the AAG nonamer. These findings with the ELA and ALG peptides led to widespread use of the ELA decamer in clinical trials for the immunological treatment of melanoma patients,[14–16] as well as regular use of the ELA decamer in more basic studies of MART-1 antigenicity.

In addition to their relevance to tumor immunology, the immunodominant epitopes from the MART-1 protein are of interest due to the very high frequency of MART-1-specific circulating CD8+ T cells in healthy HLA-A2+ individuals, as high as 1/1000 in peripheral blood.[17] Initial analysis of this repertoire in two individuals indicated that MART-1-specific T cells are clonally diverse, with no restrictions in β chain gene segment usage, and a wide diversity in CDR3 length and composition.[18,19] Although there are some exceptions as noted below, most evidence suggests that the majority of these T cells recognize both the EAA decamer and the AAG nonamer, with cross-recognition having been shown with multiple T cell clones and polyclonal populations, using both measurements of T cell effector functions and tetramer staining.[10,12,13,20–22] Indeed, T cell cross-reactivity between the EAA decamer and AAG nonamer would be crucial for mediating tumor regression upon use of the ELA peptide in cancer immunotherapy, as a quantitative analysis of peptides presented by human HLA-A2+ melanoma cells was unable to detect presentation of the EAA decamer, on which the ELA decamer is based, although presentation of the AAG nonamer was readily detected.[23]

Recently, Sliz *et al.* determined the crystallographic structures of the modified ELA decamer and the modified ALG nonamer bound to HLA-A2.[24] There was a dramatic difference in the

conformation of the peptides in these two structures, best described as a “kinked bulge” occurring in the N-terminal half of the decameric peptide. The bulge was attributed to the first and last primary anchor pockets in HLA-A2, which for both peptides consist of optimal leucine and valine side-chains, respectively. The nonamer thus has six amino acid residues between the two primary anchors, whereas the decamer has seven. The additional amino acid in the decamer forces the peptide to bulge and zig-zag just after the first primary anchor, whereas the nonamer adopts an extended conformation typical of nonameric peptides. The differences between the two structures are significant, with the backbone shift dramatically altering the surface that is presented to T cell receptors.[24,25]

On the basis of these structures and the functional data indicating that tumor-reactive CTL recognize the ELA/EAA decameric peptides well, whereas the ALG nonamer is, at best, very poorly recognized, Sliz *et al.* hypothesized that the native AAG nonamer would adopt a bulged and zig-zagged conformation similar to that of the ELA decamer. This widely accepted hypothesis provided a structural basis for cross-reactivity between the EAA/ELA decamers and the AAG nonamer. Moreover, the proposed structural similarity between the AAG nonamer and the EAA/ELA decamers explained how vaccination of melanoma patients with the ELA decamer could elicit anti-tumor immunity if only the AAG nonamer was present on the surface of melanoma cells, as suggested by the data presented by Skipper *et al.*[23]

However, efficient cross-reactivity between the EAA/ELA decamers and the native AAG nonamer is not universal. In a recent study, 15 out of 37 CTL clones efficiently lysed targets presenting the ELA decamer but not the AAG nonamer.[22] This observation could be explained by the weaker HLA-A2 binding affinity of the AAG nonamer.[26] However, rare clones have been described that show a preference for the AAG nonamer in one or more T cell effector functions.[12,21] Furthermore, the prediction that the AAG nonamer would adopt the bulged conformation is inconsistent with the database of known peptide/HLA-A2 structures, as this would require the peptide to bind with an empty P1 pocket, a binding mode that has not been observed with nonameric peptides, even when the peptide has a sub-optimal P2 anchor.[27]

Here, we report the structure of the native MART-$1_{27–35}$ AAG nonamer and a number of variants bound to HLA-A2. Inconsistent with earlier predictions, the native peptide does not adopt the bulged conformation of the ELA decamer. Rather, the peptide adopts an extended conformation nearly identical with that of the ALG nonamer. To further investigate, we determined the structures of the native MART-$1_{26–35}$ EAA decamer and the 27–35 Ala2→Leu ALG nonamer bound to HLA-A2 at a higher resolution to closely examine the dynamics of the peptide previously described by Sliz *et al.*[24] We also determined the structure of another variant, the 27(L)-35 nonamer (*L*AGIGILTV; LAG nonamer) that has been proposed as an improved melanoma vaccine candidate.[28] All MART-1 peptides and variants studied are shown in Table 1.

Overall, we find that there are two general classes of conformations for the MART-1 peptides studied: bulged or extended, the adoption of which is a function of the length of the peptide, the identity of the amino acids at the first and second position, and the physical constraints of the HLA-A2 peptide-binding groove. The bulged conformation is adopted by the EAA/ELA decamers and the LAG nonamer, whereas the extended conformation is adopted by the AAG and ALG nonamers. Thus, T cells that recognize both the AAG nonamer and the modified ELA decamer used in clinical trials and the majority of functional studies recognize peptides of two different structural classes. As noted above, clonally diverse Tcells with specificity for MART-1 are highly prevalent in HLA-A2+ individuals, indicating cross-recognition of structurally dissimilar ligands occurring on a very broad scale. Remarkably though, the previous observation that five out of five MART-1-reactive T cell clones failed to recognize the ALG nonamer, yet still responded vigorously to the AAG nonamer,[13] indicates that in

addition to being insensitive to the structural differences between the bulged and extended conformational classes, many MART-$1_{26/27–35}$-specific T cells remain sensitive to more subtle structural differences within the extended conformational class.

Our findings highlight a dichotomy of specificity and selectivity in TCR recognition of peptide/MHC. Although these properties have been shown individually before, we demonstrate here that they can operate simultaneously and, importantly, are not confined to a small number of unusual T cells, but are present in large numbers of naturally occurring T cells easily identifiable in HLA-A2+ individuals. Overall, our observations challenge our thinking about how structural information on unligated peptide/MHC complexes should be best used when addressing questions of TCR specificity. Finally, our findings indicate that caution is warranted in the design of class I MHC-based immunotherapeutics based on MART-1 tumor antigens, as neither cross-reactivity nor selectivity appears predictable based on the analysis of the structures alone.

Structures of MART-$1_{26/27–35}$-based peptide/HLA-A2 complexes reveal bulged and extended peptide conformations

Crystals of the native MART-$1_{27–35}$ nonamer (AAG nonamer) complexed with HLA-A2 were grown by screening conditions previously used to crystallize peptide/HLA-A2 complexes in our laboratory.[7,27] Crystals of the A1L-modified MART-$1_{27–35}$ nonamer (LAG nonamer), the A2L-modified nonamer (ALG nonamer), and the native MART-$1_{26–35}$ decamer (EAA decamer) complexed with HLA-A2 grew readily from these conditions, although subtle modifications resulted in improved crystals. All peptides studied are shown in Table 1. Each complex crystallized in the same space group with similar unit cell dimensions and with two molecules per asymmetric unit. Structures were solved *via* molecular replacement, using the structure of the $gp100_{209–217}$/HLA-A2 complex with the peptide/solvent atoms excluded as a search model.[27] Crystallization and refinement statistics are reported in Table 2. The structure of the ALG nonamer was determined by Sliz *et al.*,[24] and we have determined this structure at a higher resolution in order to examine more closely the potential for peptide conformational dynamics. Images showing electron density maps for each peptide in each asymmetric unit are available as Supplementary Data (Figure S1A). Also available in Supplementary Data are the initial electron density maps of the P2 side-chain regions for the first molecules in the AAG and ALG asymmetric units, calculated after the first round of TLS refinement before the peptides had been introduced (Figure S1B). These unbiased electron density maps unambiguously identify the P2 side-chains in these crystals.

Generally speaking, each complex displayed the expected peptide/class I MHC architecture, with no significant difference in the positioning of the HLA-A2 peptide-binding grooves (the average RMSD for superimpositions of the peptide binding domain is 0.35(±0.07) Å). Notably though, each of the peptides adopted one of two general conformations: the bulged and zig-zagged conformation of the ELA decamer, or the extended conformation of the ALG decamer. Inconsistent with earlier postulations,[13,24] the native AAG nonamer fell into the latter category, whereas the EAA decamer, the ELA decamer, and the LAG nonamer belong to the former. These overall conformations and their differences are summarized in Figure 1. The differences between the bulged and extended conformations are further highlighted in Supplementary Data (Figure S2) and are discussed in detail by Sliz *et al.*[24] There are no crystallographic contacts to the peptides in any of the structures.

A matrix of RMS deviations for pairwise superimpositions of the backbones of each peptide, including both molecules in each asymmetric unit, is shown in Figure 2. This analysis quantifies the simiarities and differences between the various peptides. The backbones of peptides in the extended conformation (AAG nonamer, ALG nonamer) superimpose with RMSDs between

0.19 Å and 0.77 Å, whereas the backbones of the peptides in the bulged conformation (EAA and ELA decamers, LAG nonamer) superimpose with RMSDs between 0.08 Å and 0.26 Å (the larger range for the extended conformations reflects the presence of backbone conformational heterogeneity in the extended conformation, as described below). The backbones of the two classes of peptides (bulged and extended), on the other hand, superimpose with RMSD values between 1.77 Å and 2.11 Å, reflecting the substantial differences in the center of the peptides seen in Figure 1.

It is of interest that the LAG nonamer adopts the bulged conformation of the EAA/ELA decamers, inserting leucine at position 1 into the HLA-A2 P2 pocket and leaving the P1 pocket unoccupied. As developed further below, this indicates that, at least for this peptide, the penalty of losing stabilizing N-terminal interactions with the P1 pocket is overcompensated by the gain of favorable interactions within the P2 pocket. The "empty" LAG P1 pocket is reminiscent of that seen in the structure of the octameric $Tax_{12–19}$ peptide bound to HLA-A2:[29] the pocket is fully intact, with the side-chains fully superimposable on those with the corresponding nonamers/decamers, and a water molecule is found in the position normally occupied by the P1 carbonyl oxygen atom. Additionally, a formate anion was found in the pocket of the LAG nonamer, occupying the position normally occupied by the P1 α-carbon and N-terminal nitrogen atoms and hydrogen bonding to the additional water molecule and Tyr171 of the HLA-A2 heavy chain (Supplementary Data, Figure S3).

Conformational heterogeneity in the extended but not in the bulged conformation

The peptides in the extended conformation (AAG nonamer, ALG nonamer) display a level of conformational heterogeneity not seen in the bulged conformation. For both the AAG and ALG structures, each MHC molecule in the asymmetric unit presents the peptide slightly differently. This is shown quantitatively by the RMSD values in Figure 2, and is illustrated in Figure 3. Figure 3(a) shows a superimposition of the AAG and ALG nonamers, including both molecules in each unit cell for the structures solved here, as well as the structure of the ALG nonamer solved by Sliz *et al.*[24] Differences are seen in the backbones, particularly in the central portion of the peptide, as well as the side-chains. The structure of the ALG nonamer solved here shows the greatest backbone diversity, as the backbone in the center of the peptide in the first molecule in the ALG unit cell occupies two discrete positions (MOL 1A and MOL 1B), with the alternative (MOL 1B) position occurring *via* large rotations of the Ψ angle of Ile30 (P4; rotation of 147°) and the Φ angle of Gly31 (P5; rotation of 207°). Considering both molecules in the unit cell, there is a 1.7 Å variation in the position of the Gly31 α carbon in the peptides in this structure (these two conformations were clearly discernible in the electron density; Supplementary Data, Figure S4). A consequence of the backbone shift is an almost 180° flip in the orientation of the Ile30 (P4) carbonyl oxygen and the Gly31 (P5) amide nitrogen. The conformation of the ALG nonamer of Sliz *et al.* is intermediate between the ALG conformations observed here, as illustrated in Figure 3(b). Figure 3(c) summarizes the relationships between the peptide conformations, and indicates that the diversity in the AAG and ALG structures can be summarized by the relative displacement of the Gly31 (P5) α carbon.

The conformational heterogeneity in the native AAG nonamer is smaller than that for the ALG nonamer (Figure 3(a)–(c)), with a Gly31 α carbon shift of only 0.5 Å for the two molecules in the AAG nonamer asymmetric unit, compared to 1.7 Å for ALG. The AAG conformations are bracketed by the ALG conformations: the ALG MOL 2 conformation is closest to the AAG MOL 2 conformation (Gly31 C^{α} distance of 0.1 Å, RMSD of 0.19 Å), whereas the AAG MOL 1 conformation is closest to the ALG conformation in the structure described by Sliz *et al.* (Gly31 C^{α} distance of 0.2 Å, RMSD of 0.26 Å).

Despite the conformational heterogeneity in the extended conformations, the structures do not suggest a propensity for the AAG or ALG nonamers to adopt the bulged conformation of the EAA/ELA decamers or the LAG nonamer. This is shown in Figure 3(d), in which the conformation of the ELA decamer is superimposed on the three conformations of the ALG nonamer reported here (ALG MOL 1A, ALG MOL 1B, and ALG MOL 2). It is reflected also in Figure 2, in which the RMSDs for the cross-conformation superimpositions are at or above 1.8 Å, regardless of which peptide pair is compared.

In contrast to the peptides in the extended conformation, those in the bulged conformation (EAA/ELA decamers, LAG nonamer) do not display conformational heterogeneity. This is demonstrated in Figure 3(e), which shows a superimposition of the EAA, LAG, and ELA peptides. Although some heterogeneity remains in the side-chains, as discussed below, the backbones are highly superimposable, even in the central region of the peptide. A further comparison of the peptide conformations and heterogeneity is seen in the temperature factors of the peptides, summarized in Supplementary Data, Figure S5. The greater conformational heterogeneity of the peptides in the extended conformation (AAG and ALG nonamers) is reflected in the much higher values across the centers of the peptides.

As is shown in Figure 3, the conformational heterogeneity in the extended conformation includes side-chains as well as backbones. Ile30, Ile32, and Leu33 (P4, P6, and P7) all populate multiple conformations in the AAG and ALG nonamers, and have correspondingly high temperature factors. Although there are some differences in the placement of these side-chains in these peptides, the data do not allow us to conclude directly that the Ala2→Leu substitution is responsible for any changes in side-chain conformation. For example, for Ile30 (P4), the major difference between the AAG and ALG conformations is a 70–100° rotation in the χ_2 torsion angle. Yet, the temperature factors at this position are among the highest in the AAG and ALG structures, and there are multiple conformations present in each of the extended structures, suggesting this side-chain is highly mobile in both the AAG and the ALG peptides. Interestingly, although Ile32 (P6) is buried in the HLA-A2 binding groove, it populates two distinct rotamers in both the AAG and ALG structures. Leu33 (P7) seems particularly dynamic, as its side-chain could be refined in two different conformations in the second molecule in both the AAG and ALG asymmetric units (not shown).

Unlike the extended conformation, the side-chains of Ile30 and Ile32 (P4 and P6) for the peptides in the bulged conformation (the EAA/ELA decamers and the LAG nonamer) do not display significant conformational heterogeneity or high temperature factors. The heterogeneity in Leu33 (P7) remains, however, and this position was again refined in two conformations for both molecules in the LAG asymmetric unit.

The differing levels of peptide backbone conformational heterogeneity were further investigated *via* molecular dynamics simulations. Unrestrained 30 ns simulations in explicit solvent were performed on the AAG, ALG, and ELA peptide/HLA-A2 complexes. In general, the dynamics simulations captured the crystallographic observations: the center of the ALG nonamer showed significant conformational diversity over the course of the simulation, whereas the AAG and ELA peptides were more rigid. This is shown in Figure 4(a), which compares average temperature factors for the peptide backbone units calculated over the lengths of the simulations for the three peptides. Notably, most backbone motion in the ALG peptide is found in the center of the peptide. The simulations with the ALG peptide also captured both conformations seen in the center of the peptide (MOL 1A and MOL 1B), with correlated bond rotations occurring around the Ψ angle of Ile30 (P4) and the Φ angle of Gly31 (P5) (Figure 4(b) and (c)). The alternate, “flipped” ALG conformation was observed for approximately 20% of simulation time, consistent with the crystallographic data indicating a population of less than 50%. The presence of discrete, well-populated conformations during

the simulations, apparent from the clusters in Figure 4(b), may indicate why clear electron density is observed in the crystallographic structures for each of the various ALG conformations.

No correlated Φ/Ψ bond rotation was seen with the AAG or ELA peptides (see Supplementary Data). Together then, the crystallographic and molecular dynamics data indicate that one consequence of the alanine→leucine substitution in the AAG peptide is to substantially enhance both the frequency and amplitude of molecular motion in the center of the peptide (additional details regarding the molecular dynamics simulations are available as Supplementary Data).

Cross-reactivity and selectivity towards MART-$1_{26/27–35}$ peptide variants by naturally occurring T cells and T cell receptors

Although earlier studies showed that the ALG peptide was recognized poorly, if at all, by five different MART-$1_{26/27–35}$-reactive CTL clones,13 the observation that the AAG and ALG peptides both adopt the extended conformation in the HLA-A2 binding groove suggests that it should be possible to identify T cells that cross-react between the two. To investigate this, we tested naturally occurring tumor infiltrating lymphocytes (TIL) derived from surgically resected tumors for reactivity against the MART-$1_{26/27–35}$-based peptides studied here. Functionality was assessed by assaying for reactivity to HLA-A2-expressing T2 cells pulsed with the various MART-$1_{26/27–35}$-based peptides in a cytokine secretion assay. As shown in Figure 5, we identified two TIL cell lines, JKF6 and DMF5, that responded vigorously to all of the MART-1 peptides tested, including the ALG nonamer, which was strongly recognized by the JKF6 line, albeit less than the ELA decamer. Two other tested TIL lines, 1922-W22 and 1963-F6, did not recognize the ALG nonamer well, but exhibited strong reactivity against the ELA decamer and the native AAG nonamer, a pattern similar to that observed by Valmori *et al.*[13] None of the MART-1 reactive TIL recognized the irrelevant $gp100_{209–217}$ peptide (ITDQVPFSV), nor was there any recognition of the MART-$1_{26/27–35}$ peptides by the $gp100_{209–217}$ specific T cell clone RC612. The results observed with the cross-reactive T cells indicate that, in addition to the previously demonstrated differential T-cell reactivities against AAG and ALG peptides, naturally occurring cross-reactive T cells do exist that do not distinguish between the ALG and AAG nonamers.

We next sought to confirm whether the cross-reactivity exhibited by the JKF6 and DMF5 TIL were indeed attributable to their respective T cell receptors. *In vitro* transcribed mRNA encoding each TCR α and β chain pair from either JKF6 or DMF5 was electroporated into CD8-enriched HLA-A2+ PBMC, resulting in transient MART-1-reactive TCR expression by otherwise non-reactive T cell populations.[30] TCR gene-transferred CD8+ T cells exhibited vigorous reactivity to each of the MART-$1_{26/27–35}$-derived peptides, including the ELA, AAG, and ALG peptides (Figure 5(b)). These findings confirm that the recognition of the MART-$1_{26/27–35}$ variants by JKF6 and DMF5 T cells indeed results from the molecular recognition properties of the T cells' respective TCRs.

Determinants of the conformations of MART-$1_{26/27–35}$ variants in the HLA-A2 binding groove

The crystallographic structures of the various MART-$1_{26/27–35}$ nonamers and decamers indicate that there are two general conformational classes available to these peptides: an extended conformation adopted by the AAG and ALG nonamers, and a bulged conformation adopted by the EAA/ELA decamers and the LAG nonamer. This is in contrast to the hypothesis, based upon T cell reactivity, that the AAG nonamer adopts the bulged conformation first seen with the ELA decamer.[24] This inital hypothesis has been widely accepted, as it explains the

cross-reactivity between the AAG nonamer and the EAA/ELA/LAG peptides seen with the majority of MART-1-reactive T cells. It explains also how vaccination of HLA-A2+ melanoma patients with the ELA decamer could elicit anti-tumor immune responses if only the AAG nonamer (and not the EAA decamer) is presented by HLA-A2+ melanoma cells, as suggested by the data presented by Skipper *et al.*[23]

Although it is thus contrary to previous predictions, adoption of the extended conformation by the AAG nonamer can be explained considering the contribution of the peptide N terminus to peptide binding by HLA-A2. The N terminus normally occupies the P1 pocket in HLA-A2, making multiple hydrogen bonds with the HLA-A2 heavy chain. The energetic importance of these hydrogen bonds to peptide-MHC interactions was first shown by Bouvier and Wiley, who demonstrated that chemically blocking the peptide N terminus can destabilize class I peptide/MHC complexes more so than alterations to the primary anchor residues.[31] Khan *et al.* obtained similar findings with the octameric $Tax_{12–19}$ peptide in which the P1 pocket was empty.[29] Thus, if the AAG nonamer were to adopt the bulged conformation as predicted, the P1 pocket would be empty and the P2 pocket would be occupied by a sub-optimal alanine. Together, this would result in a significant destabilization of the peptide/MHC complex. Apparently, the AAG nonamer adopts the extended conformation, maximizing the number of stabilizing interactions with HLA-A2, filling the P1 pocket and making the expected N-terminal hydrogen bonds with HLA-A2. In fact, of all the MART-$1_{26/27–35}$ structures studied, the only “unusual” conformation observed is that of the LAG nonamer, which gives up stabilizing N-terminal interactions with the HLA-A2 P1 pocket and inserts its P1 leucine into the P2 pocket, forcing the peptide to adopt the bulged conformation. The energetic cost of this trade-off is reflected in the observation that the HLA-A2 binding affinities of the AAG nonamer and LAG nonamer are approximately equivalent (see Table 1).[13]

Broad T cell cross-reactivity in the absence of structural homology and selectivity in its presence

While perhaps readily explained, the finding that the AAG nonamer adopts the extended rather than the bulged conformation complicates our understanding of the relationship between peptide/MHC structure and T cell recognition in this system in two important ways. First, while exceptions have been noted,[12,21] T cell cross-reactivity between the AAG nonamer and the EAA/ELA/LAG peptides is extremely common, having been seen with numerous T cell clones and polyclonal populations. It has been observed by measuring T cell effector functions,[10, 12,13,20,21] as well as by staining with EAA, ELA, and AAG-loaded HLA-A2 tetramers.[22] The tetramer experiments are particularly important, as they rule out simpler explanations for cross-reactivity, such as proteolysis of the ELA peptide in culture. As clonally distinct T cells with MART-1 antigen specificity are highly prevalent in HLA-A2+ individuals,[17–19,30] the aggregated data indicate broad TCR cross-reactivity occurring on structurally dissimilar ligands.

Second, the conformation of the ALG nonamer is very similar to that of the AAG nonamer, yet Valmori *et al.* found that with five different CTL clones, the AAG nonamer is a good agonist, whereas the ALG nonamer is a null ligand or a very weak agonist at best.[13] We observed a similar pattern with the 1922-W22 and 1963-F6 T cells (Figure 5). Discrimination between the AAG and ALG nonamers is surprising, given the general expectation that improving peptide-MHC binding affinity while retaining structural homology should result in improved immunogenicity.[27]

What physical mechanisms could account for widespread T cell cross-reactivity in the absence of structural homology in the case of the AAG peptides and the ELA/EAA/LAG peptides, and the lack of cross-reactivity with some T cells in the presence of structural homology in the case

of the ALG and AAG peptides? Although multiple mechanisms could be postulated, the observation of differential dynamics between the AAG and ALG peptides suggests that peptide flexibility and backbone hydrogen bonding may have key roles. In both the crystallographic structures and the molecular dynamics simulations, the ALG nonamer was found to populate an alternative conformation in which the Ile30 (P4) carbonyl oxygen and the Gly31 (P5) amide nitrogen are flipped nearly 180°. This structural shift alters hydrogen bond donor and acceptor positions in the center of the peptide that are otherwise relatively conserved between the bulged and extended conformations (Supplementary Material, Figure S3). Thus, it may be that the enhanced dynamics of the ALG peptide reduces the time the peptide spends in a conformation compatible with the hydrogen bonding requirements of most MART-$1_{26/27–35}$-specific TCRs. Roles for peptide dynamics in influencing T cell recognition have been noted,[7,32–34] and there are clear cases where elimination of key peptide-TCR hydrogen bonds substantially weakens TCR binding.[35] Although it may seem counter-intuitive that improving peptide binding affinity increases peptide conformational dynamics, similar observations have been made in a number of systems,[36–38] and our observations are consistent with emerging principles on how protein/ligand molecular motion may be redistributed or even enhanced upon binding.[39]

For the above mechanism to be operable, T cell receptors that cross-react between the bulged and extended conformations would still need to be tolerant of the structural differences in the peptides. These differences are located largely in the center and N-terminal regions of the peptides, such that all of the MART-$1_{26/27–35}$ peptides studied share a common C-terminal conformation, as shown in Figure 3(d). Thus, except for key hydrogen bonds to the center, as noted above, MART-$1_{26/27–35}$-reactive TCRs may recognize the peptides asymmetrically, focusing largely on the common C-terminal regions, as seen in recognition of the pBM1 peptide by the TCR BM3.3.[40] Indeed, this may be the mechanism used by the JKF6 and DMF5 T cells studied here, as they responded well to all of the MART-$1_{26/27–35}$ variants studied. Alternatively (or perhaps simultaneously), MART-$1_{26/27–35}$ cross-reactive T cell receptors may possess a level of structural plasticity that allows them to adapt to the different peptides.[1,7,41–45] A TCR binding mechanism whereby receptors initially engage MHC before interacting with the peptide could facilitate such adaptive binding.[46,47]

Another possible mechanism for achieving both cross-reactivity and selectivity in T cell recognition of MART-$1_{26/27–35}$ antigens is that MART-$1_{26/27–35}$-reactive T cells induce a structural shift in the AAG nonamer upon TCR binding, forcing the peptide to adopt a conformation resembling that of the EAA/ELA/LAG peptides. Such a conformational shift could be possible in the AAG nonamer due to the sub-optimal alanine at position 2, and prevented in the ALG nonamer due to the presence of leucine in the HLA-A2 P2 pocket. Significant changes in peptide conformation occurring upon TCR binding have been observed in other cases. For example, the center of the HTLV-1 $Tax_{11–19}$ peptide presented by HLA-A2 is “squished” upon binding of the A6 and B7 TCRs.[48,49] Lee *et al.* have provided evidence for a similar occurrence in TCR recognition of native and variant HIV gag epitopes presented by HLA-A2.[6] More recently, Tynan *et al.* demonstrated that an extensively bulged Epstein-Barr viral antigen is “flattened” upon TCR recognition.[50] In addition to explaining cross-reactivity towards the AAG peptide and the poor activity of the ALG peptide, this “selective conformational shift” model could explain the improved immunogenicity of the EAA/ELA/LAG peptides over the AAG nonamer, as the need to induce a shift in the peptide would be expected to translate into a weaker TCR affinity. However, the conformational change needed for the AAG nonamer to adopt the bulged structure would be unusual and unprecedented, as it would require the AAG N terminus to move up and out of the HLA-A2 P1 pocket, resulting in the loss of multiple stabilizing hydrogen bonds as described above.

When considering cross-reactivity and specificity in recognition of the MART-$1_{26/27–35}$ variants, it is worth considering the peptides used in deriving MART-$1_{26/27–35}$-reactive CTL clones. Since the demonstration that the EAA/ELA decamers are superior antigens with a group of MART-1-reactive T cells,[12,13] many studies have used the bulged ELA decamer for deriving T cell clones. While others, including the JKF6 and DMF5 T cells studied here, were elicited on the basis of their natural reactivity against their autologous melanoma tumors, it may be illuminating to study the recognition properties of T cell clones specifically established using peptides of the extended structural class (i.e. the AAG nonamer), as the potential for cross-reactivity and selectivity between the resulting clones may differ. Such differences may have consequences for the choice of strategies for immunological treatment of melanoma, particularly those involving adoptive T cell transfer,[51] and/or genetically engineered T cells expressing potent MART-1-reactive TCRs.[16]

Clearly, additional work is required to fully determine the mechanisms of TCR cross-reactivity and selectivity towards MART-1-derived tumor antigens. Regardless of the exact mechanisms, however, our findings of extensive T cell cross-reactivity in the absence of peptide/MHC structural homology and selectivity in its presence, in one of the most commonly recognized T cell epitopes in HLA-A2+ individuals, raises challenging questions about how crystallographic structures of unligated peptide/MHC complexes should best be used when addressing questions related to TCR specificity and cross-reactivity. Finally, our results highlight a danger in using unligated peptide/MHC structures as starting templates for the design of MART-$1_{26/27–35}$-based immunotherapeutics, as neither T cell cross-reactivity nor selectivity is readily predicted by examination of the peptide/HLA-A2 structures.

Protein Data Bank accession codes

Structure factors and coordinates have been deposited in the Protein Data Bank as entries 2GUO (AAG nonamer), 2GTZ (ALG nonamer), 2GTW (LAG nonamer), 2GT9 (EAA decamer).

Supplementary Material

Refer to Web version on PubMed Central for supplementary material.

Acknowledgements

We thank Alison Wojnarowicz for excellent technical assistance. This work was supported, in part, by grants RSG 05-202-01-GMC from the American Cancer Society, MCB-0448298 from the National Science Foundation, and by the Intramural Research Program of the NCI, Center for Cancer Research. Use of GM/CA CAT at the Argonne Advanced Photon Source was supported by the US Department of Energy under contract no. W-31-109-ENG-38. GM/CA CAT has been funded with funds from NCI (Y1-CO-1020) and NIGMS (Y1-GM-1104). Molecular dynamics simulations were performed on the Notre Dame Biocomplexity Computing Cluster, supported by NSF grant DBI-0420980. O.Y.B. was supported by a fellowship from the Walther Cancer Research Center.

References

1. Ding YH, Baker BM, Garboczi DN, Biddison WE, Wiley DC. Four A6-TCR/peptide/HLA-A2 structures that generate very different T cell signals are nearly identical. Immunity 1999;11:45–56. [PubMed: 10435578]
2. Kersh GJ, Miley MJ, Nelson CA, Grakoui A, Horvath S, Donermeyer DL, et al. Structural and functional consequences of altering a peptide MHC anchor residue. J Immunol 2001;166:3345–3354. [PubMed: 11207290]
3. Sharma AK, Kuhns JJ, Yan S, Friedline RH, Long B, Tisch R, Collins EJ. Class I major histocompatibility complex anchor substitutions alter the conformation of T cell receptor contacts. J Biol Chem 2001;276:21443–21449. [PubMed: 11287414]

4. Kirksey TJ, Pogue-Caley RR, Frelinger JA, Collins EJ. The structural basis for the increased immunogenicity of two HIV-reverse transcriptase peptide variant/class i major histocompatibility complexes. J Biol Chem 1999;274:37259–37264. [PubMed: 10601290]

5. Miley MJ, Messaoudi I, Metzner BM, Wu Y, Nikolich-Zugich J, Fremont DH. Structural basis for the restoration of TCR recognition of an MHC allelic variant by peptide secondary anchor substitution. J Expt Med 2004;200:1445–1454.

6. Lee JK, Stewart-Jones G, Dong T, Harlos K, Di Gleria K, Dorrell L, et al. T cell cross-reactivity and conformational changes during TCR engagement. J Expt Med 2004;200:1455–1466.

7. Gagnon SJ, Borbulevych OY, Davis-Harrison RL, Turner RV, Damirjian M, Wojnarowicz A, et al. Tcell receptor recognition via cooperative conformational plasticity. J Mol Biol 2006;363:228–243. [PubMed: 16962135]

8. Zhao R, Loftus DJ, Appella E, Collins EJ. Structural evidence of T cell xeno-reactivity in the absence of molecular mimicry. J Expt Med 1999;189:359–370.

9. Hemmer B, Vergelli M, Gran B, Ling N, Conlon P, Pinilla C, et al. Predictable TCR antigen recognition based on peptide scans leads to the identification of agonist ligands with no sequence homology. J Immunol 1998;160:3631–3636. [PubMed: 9558061]

10. Kawakami Y, Eliyahu S, Sakaguchi K, Robbins PF, Rivoltini L, Yannelli JR, et al. Identification of the immunodominant peptides of the MART-1 human melanoma antigen recognized by the majority of HLA-A2-restricted tumor infiltrating lymphocytes. J Expt Med 1994;180:347–352.

11. Rivoltini L, Kawakami Y, Sakaguchi K, Southwood S, Sette A, Robbins PF, et al. Induction of tumor-reactive CTL from peripheral blood and tumor-infiltrating lymphocytes of melanoma patients by in vitro stimulation with an immunodominant peptide of the human melanoma antigen MART-1. J Immunol 1995;154:2257–2265. [PubMed: 7868898]

12. Romero P, Gervois N, Schneider J, Escobar P, Valmori D, Pannetier C, et al. Cytolytic T lymphocyte recognition of the immunodominant HLA-A*0201-restricted Melan-A/MART-1 antigenic peptide in melanoma. J Immunol 1997;159:2366–2374. [PubMed: 9278327]

13. Valmori D, Fonteneau JF, Lizana CM, Gervois N, Lienard D, Rimoldi D, et al. Enhanced generation of specific tumor-reactive CTL in vitro by selected Melan-A/MART-1 immunodominant peptide analogues. J Immunol 1998;160:1750–1758. [PubMed: 9469433]

14. Rosenberg SA, Yang JC, Schwartzentruber DJ, Hwu P, Marincola FM, Topalian SL, et al. Immunologic and therapeutic evaluation of a synthetic peptide vaccine for the treatment of patients with metastatic melanoma. Nature Med 1998;4:321–327. [PubMed: 9500606]

15. Speiser DE, Lienard D, Rufer N, Rubio-Godoy V, Rimoldi D, Lejeune F, et al. Rapid and strong human CD8+ T cell responses to vaccination with peptide, IFA, and CpG oligodeoxynucleotide 7909. J Clin Invest 2005;115:739–746. [PubMed: 15696196]

16. Morgan RA, Dudley ME, Wunderlich JR, Hughes MS, Yang JC, Sherry RM, et al. Cancer regression in patients after transfer of genetically engineered lymphocytes. Science 2006;314:126–129. [PubMed: 16946036]

17. Pittet MJ, Valmori D, Dunbar PR, Speiser DE, Lienard D, Lejeune F, et al. High frequencies of naive Melan-A/MART-1–specific CD8+ T cells in a large proportion of human histocompatibility leukocyte antigen (HLA)-A2 individuals. J Expt Med 1999;190:705–716.

18. Dietrich PY, Walker PR, Quiquerez AL, Perrin G, Dutoit V, Lienard D, et al. Melanoma patients respond to a cytotoxic T lymphocyte-defined self-peptide with diverse and nonoverlapping T-cell receptor repertoires. Cancer Res 2001;61:2047–2054. [PubMed: 11280765]

19. Zippelius A, Pittet MJ, Batard P, Rufer N, de Smedt M, Guillaume P, et al. Thymic selection generates a large T cell pool recognizing a self-peptide in humans. J Expt Med 2002;195:485–494.

20. Rivoltini L, Squarcina P, Loftus DJ, Castelli C, Tarsini P, Mazzocchi A, et al. A superagonist variant of peptide MART1/Melan A 27–35 elicits anti-melanoma CD8+ T cells with enhanced functional characteristics: implication for more effective immunotherapy. Cancer Res 1999;59:301–306. [PubMed: 9927036]

21. Valmori D, Gervois N, Rimoldi D, Fonteneau JF, Bonelo A, Lienard D, et al. Diversity of the fine specificity displayed by HLA-A*0201-restricted CTL specific for the immunodominant Melan-A/MART-1 antigenic peptide. J Immunol 1998;161:6956–6962. [PubMed: 9862730]

22. Dutoit V, Rubio-Godoy V, Pittet MJ, Zippelius A, Dietrich PY, Legal FA, et al. Degeneracy of antigen recognition as the molecular basis for the high frequency of naive A2/Melan-A peptide multimer+ CD8+ T cells in humans. J Expt Med 2002;196:207–216.

23. Skipper JCA, Gulden PH, Hendrickson RC, Harthun N, Caldwell JA, Shabanowitz J, et al. Mass-spectrometric evaluation of HLA-A*0201-associated peptides identifies dominant naturally processed forms of CTL epitopes from MART-1 and gp100. Int J Cancer 1999;82:669–677. [PubMed: 10417764]

24. Sliz P, Michielin O, Cerottini JC, Luescher I, Romero P, Karplus M, Wiley DC. Crystal structures of two closely related but antigenically distinct HLA-A2/melanocyte-melanoma tumor-antigen peptide complexes. J Immunol 2001;167:3276–3284. [PubMed: 11544315]

25. Romero P, Valmori D, Pittet MJ, Zippelius A, Rimoldi D, Levy F, et al. Antigenicity and immunogenicity of Melan-A/MART-1 derived peptides as targets for tumor reactive CTL in human melanoma. Immunol Rev 2002;188:81–96. [PubMed: 12445283]

26. Parkhurst M, Salgaller M, Southwood S, Robbins P, Sette A, Rosenberg S, Kawakami Y. Improved induction of melanoma-reactive CTL with peptides from the melanoma antigen gp100 modified at HLA-A*0201-binding residues. J Immunol 1996;157:2539–2548. [PubMed: 8805655]

27. Borbulevych OY, Baxter TK, Yu Z, Restifo NP, Baker BM. Increased immunogenicity of an anchor-modified tumor-associated antigen is due to the enhanced stability of the peptide/MHC complex: implications for vaccine design. J Immunol 2005;174:4812–4820. [PubMed: 15814707]

28. Carrabba MG, Castelli C, Maeurer MJ, Squarcina P, Cova A, Pilla L, et al. Suboptimal activation of CD8+ T cells by melanoma-derived altered peptide ligands: role of Melan-A/MART-1 optimized analogues. Cancer Res 2003;63:1560–1567. [PubMed: 12670905]

29. Khan AR, Baker BM, Ghosh P, Biddison WE, Wiley DC. The structure and stability of an HLA-A*0201/octameric tax peptide complex with an empty conserved peptide-N-terminal binding site. J Immunol 2000;164:6398–6405. [PubMed: 10843695]

30. Johnson LA, Heemskerk B, Powell DJ Jr, Cohen CJ, Morgan RA, Dudley ME, et al. Gene transfer of tumor-reactive TCR confers both high avidity and tumor reactivity to nonreactive peripheral blood mononuclear cells and tumor-infiltrating lymphocytes. J Immunol 2006;177:6548–6559. [PubMed: 17056587]

31. Bouvier M, Wiley DC. Importance of peptide amino and carboxyl termini to the stability of MHC class I molecules. Science 1994;265:398–402. [PubMed: 8023162]

32. Hulsmeyer M, Fiorillo MT, Bettosini F, Sorrentino R, Saenger W, Ziegler A, Uchanska-Ziegler B. HLA-B27 subtype-dependent conformation of a self-peptide. J Expt Med 2004;199:271–281.

33. Pohlmann T, Bockmann RA, Grubmuller H, Uchanska-Ziegler B, Ziegler A, Alexiev U. Differential peptide dynamics is linked to MHC polymorphism. J Biol Chem 2004;279:28197–28201. [PubMed: 15084610]

34. Probst-Kepper M, Hecht HJ, Herrmann H, Janke V, Ocklenburg F, Klempnauer J, et al. Conformational restraints and flexibility of 14-meric peptides in complex with HLA-B*3501. J Immunol 2004;173:5610–5616. [PubMed: 15494511]

35. Hausmann S, Biddison WE, Smith KJ, Ding YH, Garboczi DN, Utz U, et al. Peptide recognition by two HLA-A2/Tax11-19-specific T cell clones in relationship to their MHC/peptide/TCR crystal structures. J Immunol 1999;162:5389–5397. [PubMed: 10228016]

36. Zidek L, Novotny MV, Stone MJ. Increased protein backbone conformational entropy upon hydrophobic ligand binding. Nature Struct Biol 1999;6:1118–1121. [PubMed: 10581552]

37. Fayos R, Melacini G, Newlon MG, Burns L, Scott JD, Jennings PA. Induction of flexibility through protein-protein interactions. J Biol Chem 2003;278:18581–18587. [PubMed: 12604595]

38. Arumugam S, Gao G, Patton BL, Semenchenko V, Brew K, Van Doren SR. Increased backbone mobility in [beta]-barrel enhances entropy gain driving binding of N-TIMP-1 to MMP-3. J Mol Biol 2003;327:719–734. [PubMed: 12634064]

39. Grunberg R, Nilges M, Leckner J. Flexibility and conformational entropy in protein-protein binding. Structure 2006;14:683–693. [PubMed: 16615910]

40. Reiser JB, Darnault C, Guimezanes A, Grégoire C, Mosser T, Schmitt-Verhulst AM, et al. Crystal structure of a T cell receptor bound to an allogeneic MHC molecule. Nature Immunol 2000;1:291–297. [PubMed: 11017099]

41. Garcia KC, Degano M, Pease LR, Huang M, Peterson PA, Teyton L, Wilson IA. Structural basis of plasticity in T cell receptor recognition of a self peptide-MHC antigen. Science 1998;279:1166–1172. [PubMed: 9469799]

42. Garcia KC, Degano M, Stanfield RL, Brunmark A, Jackson MR, Peterson PA, et al. An alphabeta T cell receptor structure at 2.5 Å and its orientation in the TCR-MHC complex. Science 1996;274:209–219. [PubMed: 8824178]

43. Reiser JB, Gregoire C, Darnault C, Mosser T, Guimezanes A, Schmitt-Verhulst AM, et al. AT cell receptor CDR3beta loop undergoes conformational changes of unprecedented magnitude upon binding to a peptide/MHC class I complex. Immunity 2002;16:345–354. [PubMed: 11911820]

44. Reiser JB, Darnault C, Gregoire C, Mosser T, Mazza G, Kearney A, et al. CDR3 loop flexibility contributes to the degeneracy of TCR recognition. Nature Immunol 2003;4:241–247. [PubMed: 12563259]

45. Mazza C, Auphan-Anezin N, Gregoire C, Guimezanes A, Kellenberger C, Roussel A, et al. How much can a T-cell antigen receptor adapt to structurally distinct antigenic peptides? EMBO J 2007;26:1972–1983. [PubMed: 17363906]

46. Wu LC, Tuot DS, Lyons DS, Garcia KC, Davis MM. Two-step binding mechanism for T-cell receptor recognition of peptide MHC. Nature 2002;418:552–556. [PubMed: 12152083]

47. Boniface JJ, Reich Z, Lyons DS, Davis MM. Thermodynamics of T cell receptor binding to peptide-MHC: evidence for a general mechanism of molecular scanning. Proc Natl Acad Sci USA 1999;96:11446–11451. [PubMed: 10500196]

48. Garboczi DN, Ghosh P, Utz U, Fan QR, Biddison WE, Wiley DC. Structure of the complex between human T-cell receptor, viral peptide and HLA-A2. Nature 1996;384:134–141. [PubMed: 8906788]

49. Ding YH, Smith KJ, Garboczi DN, Utz U, Biddison WE, Wiley DC. Two human T cell receptors bind in a similar diagonal mode to the HLA-A2/Tax peptide complex using different TCR amino acids. Immunity 1998;8:403–411. [PubMed: 9586631]

50. Tynan FE, Reid HH, Kjer-Nielsen L, Miles JJ, Wilce MCJ, Kostenko L, et al. A T cell receptor flattens a bulged antigenic peptide presented by a major histocompatibility complex class I molecule. Nature Immunol 2007;8:268–276. [PubMed: 17259989]

51. Vignard V, Lemercier B, Lim A, Pandolfino MC, Guilloux Y, Khammari A, et al. Adoptive transfer of tumor-reactive Melan-A-specific CTL clones in melanoma patients is followed by increased frequencies of additional Melan-A-specific T cells. J Immunol 2005;175:4797–4805. [PubMed: 16177129]

52. Garboczi DN, Hung DT, Wiley DC. HLA-A2-peptide complexes: refolding and crystallization of molecules expressed in Escherichia coli and complexed with single antigenic peptides. Proc Natl Acad Sci USA 1992;89:3429–3433. [PubMed: 1565634]

53. Otwinowski Z, Minor W. Processing of X-ray diffraction data collected in oscillation mode. Methods Enzymol 1997;276:307–326.

54. Murshudov GN, Vagin AA, Dodson EJ. Refinement of macromolecular structures by the maximum-likelihood method. Acta Crystallog sect D 1997;53:240–255.

55. McRee DE. XtalView/Xfit – a versatile program for manipulating atomic coordinates and electron density. J Struct Biol 1999;125:156–165. [PubMed: 10222271]

56. Laskowski RA, Moss DS, Thornton JM. Main-chain bond lengths and bond angles in protein structures. J Mol Biol 1993;231:1049–1067. [PubMed: 8515464]

57. Rodriguez R, Chinea G, Lopez N, Pons T, Vriend G. Homology modeling, model and software evaluation: three related resources. Bioinformatics 1998;14:523–528. [PubMed: 9694991]

Abbreviations used

MHC

major histocompatibility complex

TIL

tumor infiltrating lymphocytes

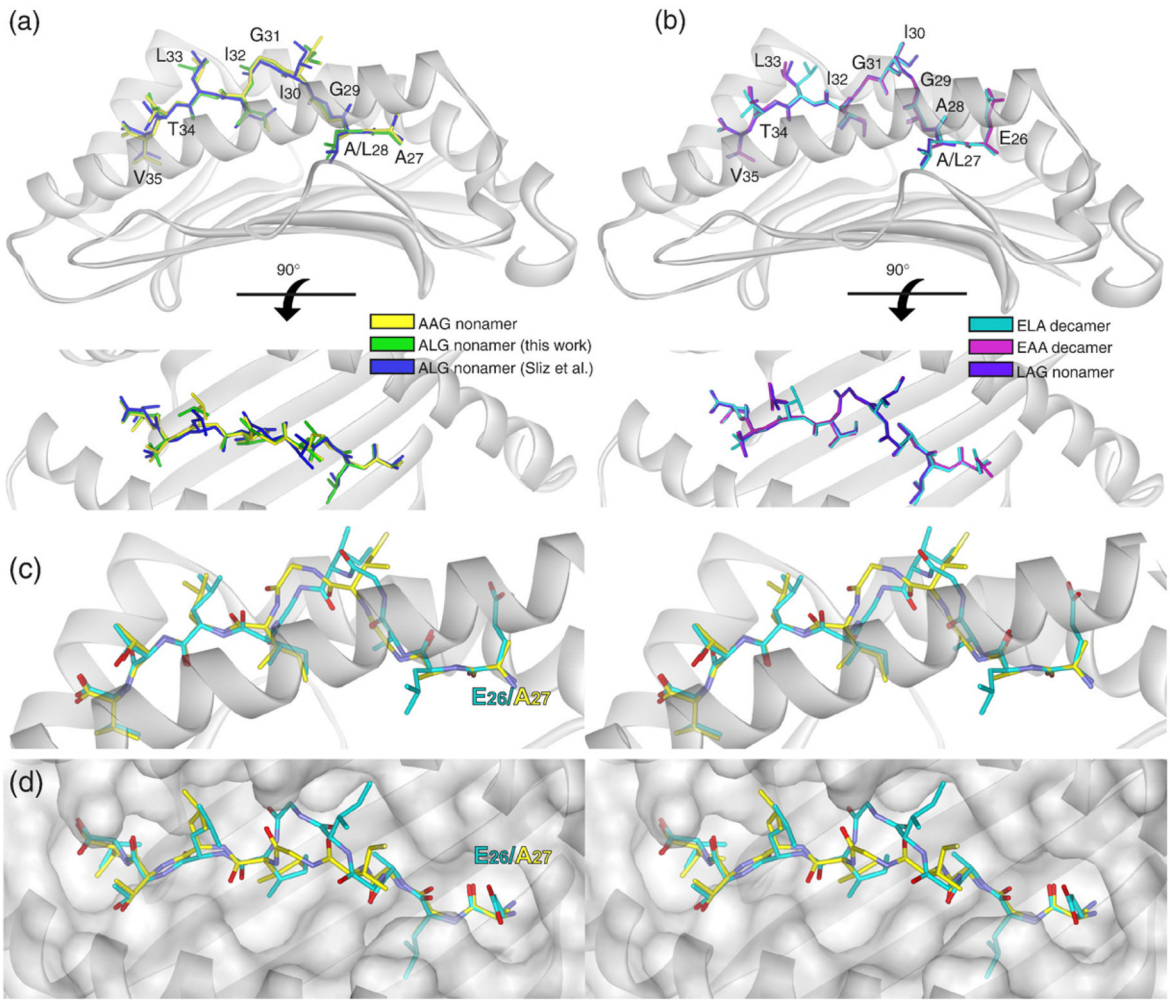

Figure 1.

MART-$1_{26/27–35}$-based peptides adopt one of two general conformations in the HLA-A2 peptide-binding groove. (a) Superimposition of the native AAG nonamer and the P2-modified ALG nonamer solved here and by Sliz *et al.*,[24] identifying the extended conformation. (b) Superimposition of the native EAA decamer, the P2-modified ELA decamer solved by Sliz *et al.*, and the P1-modified LAG nonamer, identifying the bulged conformation. (c) Stereo image comparing the extended conformation of the native AAG nonamer and the bulged conformation of the ELA decamer. (d) Same as in (c), but rotated 90° out and showing the surface of HLA-A2 as partially transparent. All superimpositions are *via* the backbones of P1 and P6–P9.

		Native AAG nonamer		ALG nonamer				LAG nonamer		EAA decamer		ELA decamer
		Mol 1	Mol 2	Sliz et al	Mol 1A	Mol 1B	Mol 2	Mol 1	Mol 2	Mol 1	Mol 2	Sliz et al
Native AAG nonamer	Mol 1		0.29	0.26	0.33	0.65	0.31	2.01	1.98	1.90	1.89	1.89
	Mol 2	0.29		0.44	0.54	0.77	0.19	2.11	2.08	2.01	2.00	2.01
	Sliz et al	0.26	0.44		0.22	0.61	0.41	1.99	1.96	1.88	1.87	1.87
ALG nonamer	Mol 1A	0.33	0.54	0.22		0.55	0.51	1.89	1.86	1.78	1.77	1.78
	Mol 1B	0.65	0.77	0.61	0.55		0.75	2.01	1.95	1.87	1.86	1.86
	Mol 2	0.31	0.19	0.41	0.51	0.75		2.06	2.04	1.97	1.96	1.97
LAG nonamer	Mol 1	2.01	2.11	1.99	1.89	2.01	2.06		0.14	0.21	0.26	0.25
	Mol 2	1.98	2.08	1.96	1.86	1.95	2.04	0.14		0.16	0.17	0.18
EAA decamer	Mol 1	1.90	2.01	1.88	1.78	1.87	1.97	0.21	0.16		0.08	0.15
	Mol 2	1.89	2.00	1.87	1.77	1.86	1.96	0.26	0.17	0.08		0.14
ELA decamer	Sliz et al	1.89	2.01	1.87	1.78	1.86	1.97	0.25	0.18	0.15	0.14	

Figure 2.

Quantitative comparison of the conformations of the various MART-$1_{26/27–35}$-based peptides. The Figure shows the pair-wise superimposition matrix of all conformations of the peptides, including both molecules in each asymmetric unit for the structures solved here (MOL 1 and MOL 2), the two alternative conformations for the ALG nonamer (MOL 1A and MOL 1B), and the ALG and ELA structures of Sliz *et al*.[24] Values are RMSD in Å. Superimpositions are *via* the backbones of P1–P9 (the first amino acid residue in the decameric peptides is P0). Values for peptides in the extended conformation (AAG and ALG) are green; values for peptides in the bulged conformation (EAA, ELA, and LAG) are blue. Cross-conformational superimpositions are red. Superimpositions of two molecules in the asymmetric units of any one structure (i.e. MOL 1 onto MOL 2) are shaded grey. It is of note that the cross-conformational superimpositions are all close to 2 Å, reflecting the differences between the bulged and extended conformations.

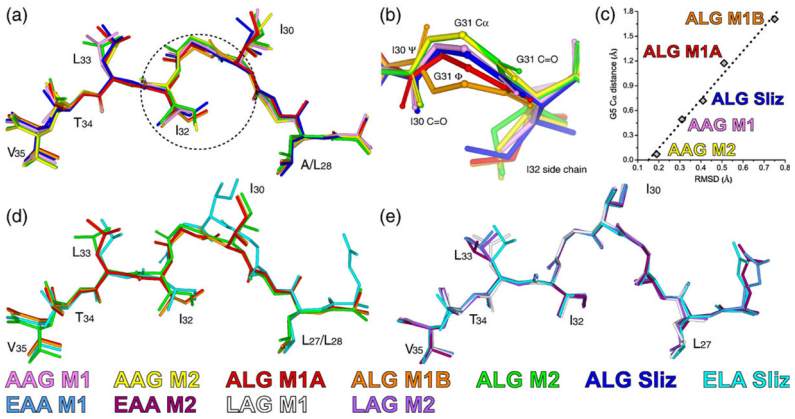

Figure 3.

Conformational heterogeneity in the extended but not the bulged conformation. (a) Superimposition of all copies of the peptides in the extended conformation reveals conformational heterogeneity, particularly in the center of the peptide. (b) Close-up of the circled region in (a), rotated 180° around the vertical axis. The diversity in the position of the backbone at Gly31 is apparent, particularly the alternative conformation of the ALG nonamer (MOL 1B). (c) The conformational heterogeneity in the extended conformation can be accounted for mostly by considering the shift in the Gly31 α carbon atom. RMSD values from Figure 2 are plotted against the shift in the Gly31 α carbon atom relative to its position in ALG MOL 2 (green in (b)). (d) The conformational heterogeneity in the extended conformation does not indicate a propensity for the peptides to adopt the bulged conformation. All conformations of the ALG nonamer, which has the greatest conformational heterogeneity, are superimposed onto the conformation of the ELA decamer. (e) Superimposition of all copies of the peptides in the bulged conformation. All superimpositions are *via* the backbones of P1 and P6–P9.

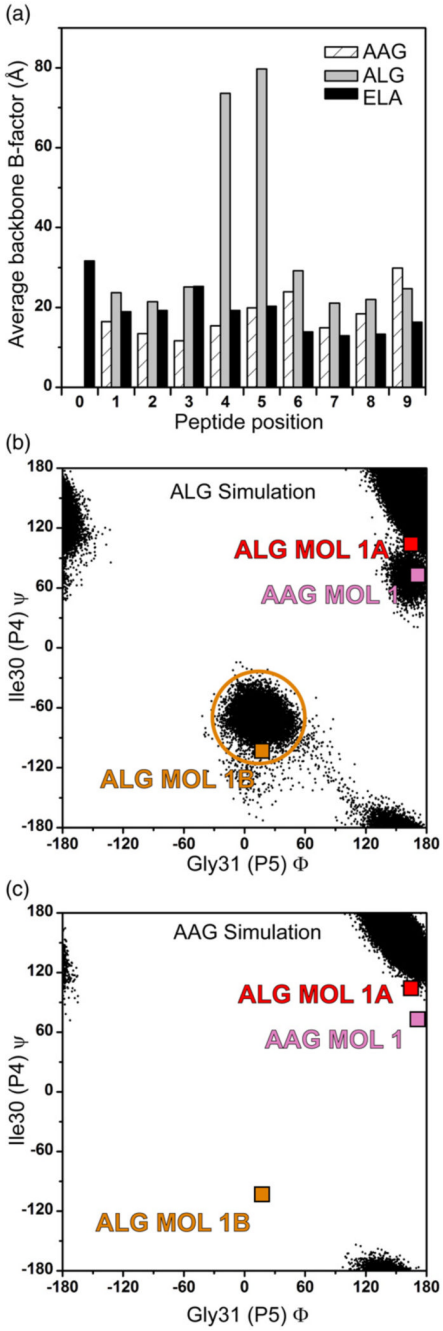

Figure 4.

Molecular dynamic simulations indicate the ALG nonamer is mobile within the HLA-A2 peptide-binding groove. (a) *B*-factors averaged for each peptide backbone unit (N, CA, C, and O) computed from unrestrained, 30 ns molecular dynamic simulations of the AAG, ALG, and ELA peptide/HLA-A2 complexes indicates that the center of the ALG nonamer is highly mobile compared to the AAG and ELA peptides. (b) During the ALG nonamer simulation, the center of the peptide was found to populate a conformation similar to the alternative, “flipped” conformation observed crystallographically. This is demonstrated by plotting the Ψ angle of Ile30 (P4) *versus* the Φ angle of Gly31 (P5) for each step in the simulation and comparing the results with the crystallographically observed Φ/Ψ angles (indicated in the plot). The

alternative, flipped conformation similar to that observed in ALG MOL 1B (circled in (b)) was observed for approximately 20% of simulation time. (c) In contrast to the ALG nonamer, the AAG nonamer did not adopt the alternative conformation, instead maintaining a conformation close to the single conformation observed crystallographically. For molecular dynamic simulations with the ALG and ELA peptide/HLA-A2 complexes, starting coordinates were from the structures described by Sliz *et al.*[24] For the AAG simulations, starting coordinates were from the second molecule in the asymmetric unit (chains D, E, and F) from the structure reported here. Hydrogen atoms were added to the starting structures using the Protonate tool of the AMBER 8 suite [http://www.amber.scripps.edu]. Using the xLEaP tool, the structures were immersed in TIP3P water boxes such that no protein atoms were less than 12 Å from any side. Sodium cations were added for neutrality. This resulted in systems consisting of 19,567 atoms for the AAG system, 21,350 atoms for the ALG system, and 18,142 atoms for the ELA system. Dynamics simulations were then performed using the PMEMD module, with parameters from the parm99 set. Equilibration consisted of 10,000 steps of conjugate gradient energy minimization, followed by 20 ps of MD with restraints applied to the proteins to equilibrate the water. A series of energy minimizations was then carried out to relax the proteins, whereby the restraints were eliminated gradually. The systems were then warmed to 300 K over three MD simulations for a total of 480 ps of dynamics. This was followed by unrestrained production runs of 30 ns. The SHAKE algorithm was used, allowing a 2 fs time-step. Long-range electrostatics were treated *via* particle mesh Ewald. Trajectory analysis was carried out with the Ptraj tool and in-house scripts.

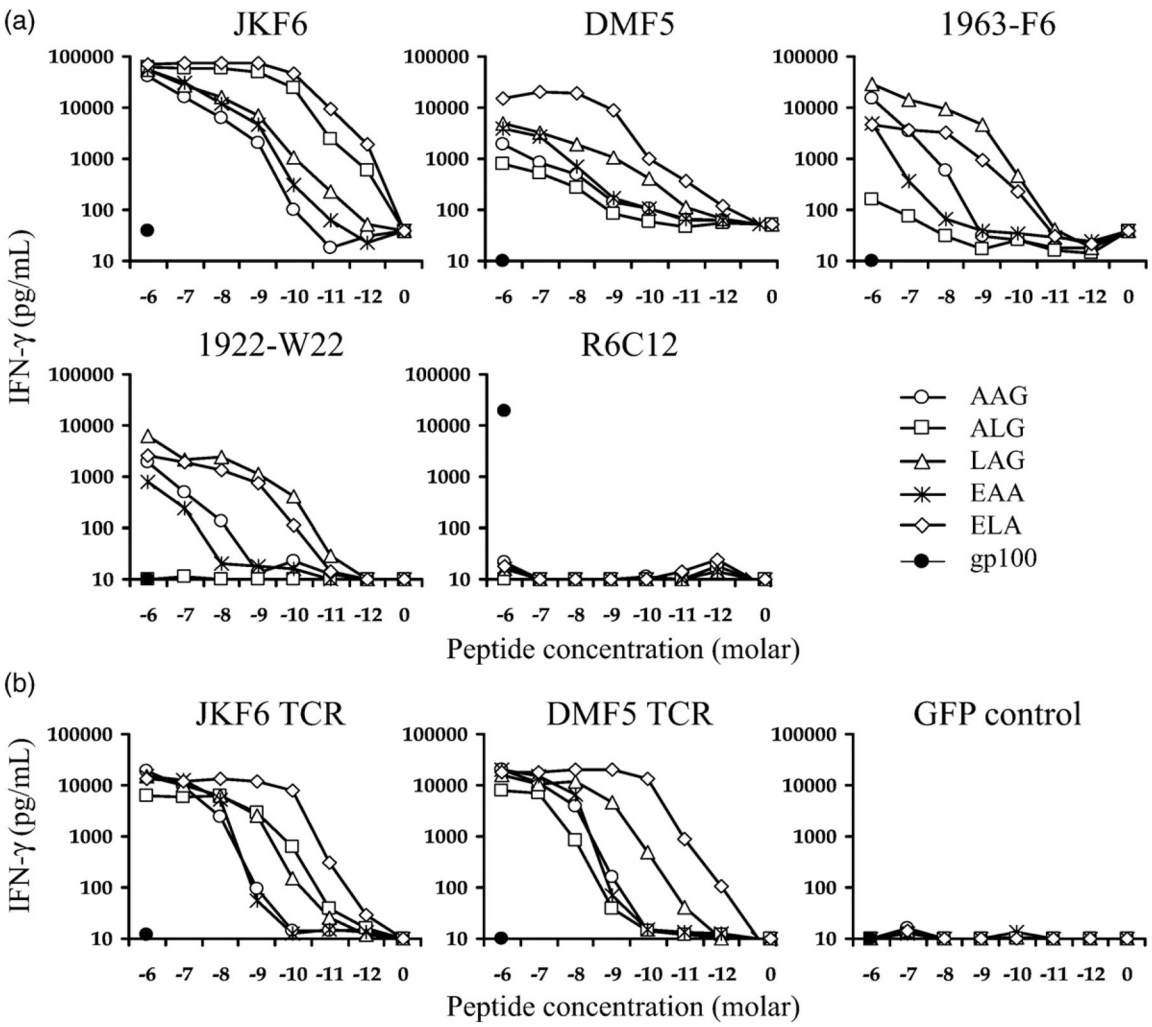

Figure 5.

Cross-reactivity and specificity towards MART-$1_{26/27–35}$ variants with naturally occurring TIL and TCR RNA-electroporated PBL. (a) Four naturally occurring MART-$1_{27–35}$ reactive TIL (JKF6, DMF5, 1963-F6, 1992-W22) and the $gp100_{209–217}$-specific T cell clone R6C12, were assayed for reactivity towards T2 APC pulsed with the MART-$1_{26/27–35}$ peptide variants or the $gp100_{209–217}$ negative control peptide. JKF6 and DMF5 recognized all of the MART-$1_{26/27–35}$ variants studied, including the ALG nonamer. Similar to the findings reported by Valmori *et al.*,[13] 1963-F6 and 1922-W22 recognized the ALG nonamer either very poorly or not at all, despite the observation that the peptide adopts the same overall structure as the AAG nonamer. (b) Gene transfer of MART-1-specific TCR α and β chains from either the JKF6 and DMF5 T cells confers reactivity towards the MART-$1_{26/27–35}$ variants to otherwise non-reactive CD8+ PBL. TCR gene-transduced CD8+ T cells did not recognize the $gp100_{209–217}$ negative control peptide. For cytokine secretion assays, cryopreserved TIL samples were thawed and cultured overnight in culture medium plus rhIL-2 (50 CU/ml). Responder cells were washed twice, plated at 1×10^5 cells, then co-cultured overnight with 1×10^5 HLA-A2+ T2 APC unpulsed or pulsed with titered concentrations of the AAG, ALG, LAG, EAA or ELA peptides or 1 μM $gp100_{209–217}$ peptide. Co-culture supernatants were harvested and assessed for the presence of IFN-γ by ELISA assay in accordance with the manufacturer's protocol (Pierce Endogen). Values reflect the mean of duplicate measurements

and are reported in pg/ml. For TCR gene isolation, RNA was purified from T cell clones using Qiagen RNEasy. 5′RACE was performed using BD SmartRace, using the universal 5′ primer, and a 3′ gene-specific primer for the TCR α constant region, or C1 or C2 β constant regions. Products were separated by electrophoresis and appropriately sized bands were excised, subcloned into pCR2.1 (Invitrogen) vector, and sequenced. For *in vitro* TCR RNA transcription and expression in PBMC, gene-specific oligonucleotide primers were generated for the production of *in vitro* RNA transcription (IVT). The 5′ primer included the bacteriophage T7 polymerase binding sequence, followed immediately by a Kozak sequence, a start codon and the next 19–25 bp of Vα or Vβ region for each TCR gene; JKF6 TRVB28, DMF5 TRVB6.4. Vα regions were all 12.2 fwd 5′ TAATAC GAC TCA CTA TAG GGA GAA CCG CCA GCA AAT CCT TGA GAG GTT TAC 3′.[30] Reverse primers included 64T and 18–25 bp of the relevant α or β constant region sequence. Reverse primers were Cα 5′ (64)T TTC AAC TGG ACC ACA GCC TCA GC 3′; C1-β 5′ (64)T TTC ATG AAT TCT TTC TTT TCA CC 3′ or C2-β 5′ (64)T TCT AGC CTC TGG AAT CCT TTC TCT TG 3′. For IVT, a PCR product was generated using the subcloned cDNA in pCR2.1 as template with the above oligonucleotide primer sets. Resulting bands were gel-purified and used for a second round of PCR amplification. PCR product was cleaned using Zymogen DNA purification columns. A 1–3 μg sample of PCR product was used as template for IVT using Ambion T7 mMESSAGE MACHINE according to the manufacturer's instructions, followed by RNA cleanup using Qiagen RNEasy. In preparation for RNA electroporation, donor TIL or PBMC from phereses were stimulated *in vitro* with 50 ng/ml OKT-3, 50 CU IL-2 in STEM:RPMI medium for three days, when CD8+ cells were positively selected using Miltenyi Biotech microbeads and magnetic columns. PBMC were then grown *in vitro* an additional 2–15 days in IL-2-containing medium before use. For TCR electroporation, 2.0 μg of RNA from each TCR gene was used per 1×10^6 cells at 2.5×10^7 cells/ml in Opti-MEM serum-free medium (Invitrogen). Cells were rested for 2 h without IL-2 post-electroporation before use in FACS staining or co-culture experiments.

Table 1

MART-$1_{26/27–35}$-based peptides

MART-1 residue number **Peptide position**	**26** **P0**	**27** **P1**	**28** **P2**	**29** **P3**	**30** **P4**	**31** **P5**	**32** **P6**	**33** **P7**	**34** **P8**	**35** **P9**	**HLA-A2 binding affinity relative to AAG**[a]
Native AAG nonamer		A	A	G	I	G	I	L	T	V	1
Modified ALG nonamer		A	**L**	G	I	G	I	L	T	V	40
Modified LAG nonamer		**L**	A	G	I	G	I	L	T	V	1
Native EAA decamer	E	A	A	G	I	G	I	L	T	V	4
Modified ELA decamer	E	**L**	A	G	I	G	I	L	T	V	9

[a]Binding data are taken from Valmori *et al.*[13] The numbers are the *n*-fold improvement in HLA-A2 binding affinity relative to the AAG nonamer.

Table 2

X-ray data and refinement statistics

Complex	AAG	ALG	LAG	EAA
Source	APS 23ID	APS 23ID	APS 23ID	APS 23ID
Space group	$P2_1$	$P2_1$	$P2_1$	$P2_1$
Unit cell parameters				
a (Å)	83.96	58.40	58.31	58.34
b (Å)	58.37	84.31	84.27	84.18
c (Å)	89.43	84.14	84.29	84.06
β (deg.)	109.66	90.13	90.11	90.08
Molecules/a.u.	2	2	2	2
Resolution (Å)	20–1.9	20–1.7	20–1.55	20–1.75
Total unique reflections	62,984	87,480	110,393	78,249
Mosaicity (deg.)	0.52	0.37	0.42	0.37
Completeness (%)	96.4 (87.9)	97.0 (85.6)	93.2 (67.8)	94.9 (71.5)
I/σ	14.2 (2.5)	13.1 (2.1)	14.8 (2.1)	14.0 (2.3)
R_{merge} (%)	10.7 (46.3)	10.0 (47.9)	10.8 (35.4)	9.9 (36.3)
Average redundancy	3.0 (2.4)	3.5 (2.6)	3.1 (1.5)	3.1 (2.1)
R_{work} (%) (no. reflections)	18.7 (59,801)	17.2 (83,098)	18.1 (104,852)	17.1 (74,349)
R_{free} (%) (no. reflections)	24.4 (3183)	21.7 (4382)	21.8 (5541)	21.3 (3900)
Average *B*-factor (peptide) ($Å^2$)	15.4 (22.8)	21.7 (26.7)	22.1 (24.2)	20.1 (20.7)
Ramachandran plot				
Most favored (%)	91.7	92.6	92.9	92.8
Allowed (%)	8.0	7.1	6.8	6.9
Generously allowed (%)	0.3	0.3	0.3	0.3
RMS deviation from ideality				
Bond lengths (Å)	0.017	0.016	0.016	0.015
Bond angles (deg.)	1.764	1.710	1.730	1.636
Coordinate error (Å)	0.11	0.08	0.06	0.08
PDB ID	2GUO	2GTZ	2GTW	2GT9

HLA-A2 was produced by refolding bacterially expressed soluble HLA-A2 andβ_2m inclusion bodies in the presence of excess peptide[52]. Refolded protein was purified *via* ion exchange and size-exclusion chromatography. Peptides were synthesized locally on an ABI 433A instrument; purity and identity were confirmed by HPLC and ES mass spectrometry. Peptide/HLA-A2 crystals were grown using 24% PEG 3350 as a precipitant in 25 mM Mes (pH 6.5) with the addition of 0.1 M sodium chloride (AAG and EAA), 0.1 M ammonium chloride (ALG) or 0.1 M potassium acetate (LAG) by the sitting-drop, vapor-diffusion method. Streak-seeding was used to improve quality. Crystals were transferred to 30% (w/v) PEG 3350, 20% (v/v) glycerol for cryoprotection for several seconds and frozen in liquid nitrogen. Data reduction was performed with HKL2000.[53] Structures were solved by molecular replacement with MOLREP from CCP4 using the gp100$_{209}$/HLA-A2 structure as a search model with the coordinates for the peptide and solvent removed.[27] Clear MR solutions were obtained in all cases; correlation coefficients and initial *R*-factors were 0.80–0.81 and 0.28–0.29. Rigid body refinement followed by TLS refinement and multiple steps of restrained refinement were performed with Refmac5.54 Anisotropic and bulk solvent corrections were taken into account throughout refinement. After TLS refinement, the peptides could be clearly positioned using $2F_O–F_C$ maps. Water molecules were added using ARP/wARP.[54] Graphical evaluation of the models and fitting to maps were performed using XtalView.[55] Procheck[56] and the WHATIF server[57] were used to evaluate the quality of the structures during and after refinement. Unless otherwise indicated, numbers in parentheses refer to the highest resolution shell. Coordinate error is the mean estimate based on maximum likelihood methods.